EXPERIMENTAL STUDY OF FLUID FORCES ON WHIRLING CENTRIFUGAL IMPELLER IN VANELESS DIFFUSER

H. Ohashi, Professor, H. Shoji, Lecturer
S. Yanagisawa, Graduate Student* and K. Tomita, Graduate Student**
University of Tokyo
Tokyo, Japan

ABSTRACT

Fluid forces on a rotating centrifugal impeller in whirling motion were studied experimentally. The test was limited to the cases in which a two-dimensional impeller surrounded by an unbounded vaneless diffuser whirls on a circular orbit with various positive and negative angular velocities. The results showed that the fluid forces exert a damping effect on the rotor whirl in most practically significant cases. Calculations were also conducted for pumps with the same geometry and whirl condition as those in the experiment for shock-free entry conditions. Quantitative agreement was obtained for the tangential component of fluid forces in positive whirl, but other quantities could be predicted only qualitatively.

NOMENCLATURE

a = conversion factor, N/V
b = vane width, m
d = impeller diameter, m
E = output of load cell, V
f = normalized fluid force
F = fluid force on impeller vanes, N
H = total head rise, m
Q = flow rate, m^3/s
u = peripheral speed, m/s
β = vane angle to radius
ε = eccentricity of whirl, m
θ = phase angle of whirl
ρ = density of fluid, kg/m^3
ϕ = flow coefficient
ψ = head coefficient
ω = angular velocity of pump shaft, rad/s
Ω = angular velocity of whirl, rad/s

Subscript
r,θ: radial and tangential component
sf : shock-free entry condition
2 : impeller exit

INTRODUCTION

Recent advances in rotor dynamics made it possible to analyse very complex shaft system of multi-stage pumps and compressors. In these analyses unsteady hydrodynamic forces acting on each rotor element like bearing, seal ring, balance piston and impeller, play a predominant role in the stabilization or destabilization of rotor whirl.

As to fluid forces acting on a centrifugal impeller of pumps and compressors, many contributions [1,2] have been done to the steady lateral forces (radial thrust), which occur either by azimuthally asymmetric configuration of volute casing or by misalignment of impeller and guide vanes.

To the contrary, limited studies [3,4] have been published on the unsteady part of lateral forces, which is induced by the whirling motion of rotating impellers. This is the very information sought for the improvement of stability analysis.

Chamieh and Acosta [4] applied an actuator disc model to the calculation of lateral forces on a whirling centrifugal impeller in an unbounded vaneless diffuser. This analysis succeeded in evaluating fluid forces normal to the whirling velocity (radial component), but led to the somewhat unnatural conclusion that there were no fluid forces parallel to the whirling velocity (tangential component), that is, the fluid forces remained always neutral to the stability of the whirling rotor.

Thompson [5] treated also the case of an unbounded centrifugal impeller. Under the assumption of quasi-steady flow, the perturbed flow in each impeller passage was solved by a computer program using a streamline curvature method. This method was applied to several industrial compressors and proved that whirl-exciting tangential forces did indeed occur with some impeller designs. No generalized guidelines, however, have been established by this method, and the question remains still unanswered whether the quasi-steady assumption is realistic under these circumstances.

Colding-Jorgensen [6] calculated the fluid forces on a whirling centrifugal impeller in a spiral volute casing under the assumption of quasi-steady flow. In this analysis, the casing was replaced by distributed vortices, and the impeller by a point source with constant circulation. Although the theory succeeded in determining the stiffness and damping coefficients of fluid forces in directly applicable form, the quantitative validity of the result must be carefully checked, because the impeller was represented by a too simplified model.

Recently two of the present authors treated analytically the case of a whirling centrifugal impeller in an unbounded vaneless diffuser [7]. This analysis was based on the singularity method for unsteady potential flow, and the interactions between impeller vanes and shed vortices were taken into consideration. Sample calculations were performed for various values of whirl speed, vane angle and number of vanes. The result showed that the fluid forces exerted damping effect throughout the surveyed range of parameters both in positive and negative whirl.

The present experimental study is the direct counterpart to the above mentioned theoretical study. Therefore the geometries of the test impeller and casing were determined to be similar to those of sample calculation. This is the reason why this experiment adopted deliberately much simpler configurations than those in actual pumps and compressors. This study will be extended to more realistic configurations, for example, an impeller in a vaned diffuser or in a spiral volute casing, after the present series for vaneless diffuser are completed.

Experimental study on this subject is quite rare. A recent report by Brennen et al. [8] revealed that a

* Present affiliation, Hitachi, Ltd.; ** Ministry of International Trade and Industry.

test program for the measurement of whirl-excitation forces in a centrifugal pump with volute casing is under way at California Institute of Technology. The stress of this program seems to be laid on a more practical side than we intend, because the adopted impeller/casing configuration is scaled to high-performance industrial pumps

TEST FACILITY

The overall arrangement of the test facility is illustrated in Fig.1. The test pump is a single-stage, vertical shaft, centrifugal type, and the facility is composed of three major sections; a water recirculating loop, an eccentric drive mechanism and a measuring system.

The test impeller ③ introduces water from a settling tank ① via a suction pipe ②. The discharged flow proceeds to a vaneless diffuser ④, passes through a wire gauze in order to ensure azimuthally uniform outflow, and returns to the settling tank via two separate pipes ⑤ with flow regulating valves ⑥.

Two test impellers (A and B) are identical except for the vane angle. They are made of aluminum to reduce the inertia force resulting from the whirling motion. Six vanes with logarithmic spiral form are installed between parallel front and back shrouds, thus constituting a two-dimensional impeller. Principal dimensions of the impellers and the diffuser are listed in Table 1.

For sealing of the whirling pump shaft, a specially designed multi-disc controlled gap sealbox ⑧ is installed, which allows radial displacement of rotating shaft with minimum hydraulic reaction and leakage (see Fig.2).

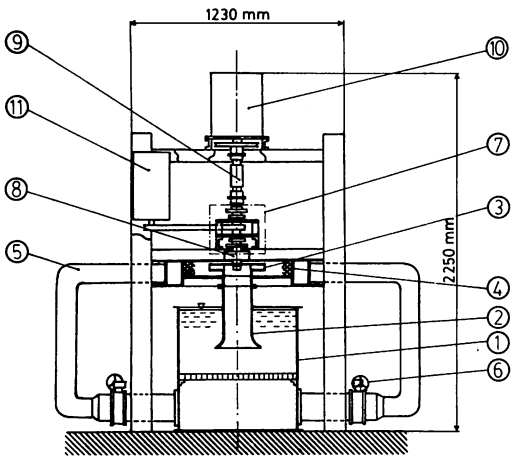

1; settling tank
2; suction pipe
3; test impeller
4; vaneless diffuser with wire gauze at exit
5; two return pipes
6; two butterfly valves
7; eccentric drive mechanism
8; multi-disc shaft seal
9; flexible coupling
10; main drive motor
11; eccentric drive motor

Fig.1 Test facility

The mechanism of the eccentric drive is illustrated schematically in Fig.2. The impeller is supported overhung by two ball bearings, which are mounted separately on the upper and lower whirl plates. These plates are then forced into whirling motion by means of a couple of eccentric drive shafts with variable eccentricity ε . These shafts are driven in synchronism by a variable speed motor ⑪ through a cogged belt. The angular velocity of whirl, Ω, can be adjusted continuously by the speed control of this motor.

The pump shaft is driven by a main motor ⑩ , and the relative movement between pump and motor shafts is absorbed by a spring-type flexible coupling ⑨. The angular velocity of the pump shaft, ω, is kept constant throughout the experiment (ω = 60.3 rad/s (9.60 Hz)).

Fluid forces acting on the impeller are evaluated from the reaction forces acting on the lower bearing. As seen from Fig.2, the outer race of the lower bearing is attached to the lower whirl plate through four load cells arranged with 90° angle difference (x- and y-direction).

Table 1 Principal dimensions

Impeller	Two-dimensional, closed type
outer diameter d_2	350 mm (13.8 inch)
inner diameter d_1	175 mm (6.89 inch)
vane width b	35 mm (1.38 inch)
suction dia. d_s	160 mm (6.30 inch)
number of vanes	6
vane angle β (angle to radius)	68° for impeller A, 60° for impeller B (logarithmic spiral)
Diffuser	Vaneless, parallel walled
exit diameter d_3	700 mm (27.6 inch)
wire gauze	40 mesh per inch, 51 % open area
width	70 mm (2.76 inch)
Return pipe diameter	Double outlets, axi-symmetric 100 mm (3.94 inch)

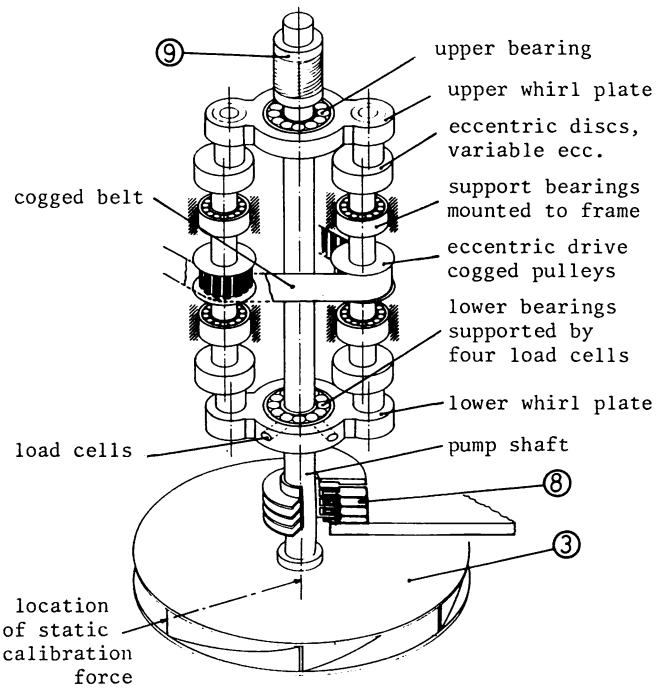

Fig.2 Details of eccentric drive mechanism

The outputs of the four load cells, together with phase angle signals from the pump and eccentric drive shafts, are stored on an analog data recorder. In order to eliminate high frequency noise, a low pass filter (cut-off frequency = 100 Hz) is applied before recording. All records are then computer processed, after having been digitized at 1 ms sampling rate.

DATA EVALUATION

Calibration

The load cells were calibrated by applying known static forces (maximum 147 N (33 lbf)) to the impeller shaft at the point corresponding to the center hight of vanes (see Fig.2). The conversion factors (a; impeller force (N)/load cell output (V)) were determined for the x- and y- direction separately. The linearity of the cells were satisfactory and all cross terms, output of y-cells to x-directed force for instance, remained less than two percent of their principal terms.

Evaluation of Fluid Forces on Impeller Vanes

The object of this experiment is to obtain experimental data, which can be directly compared with the corresponding theoretical results [7]. Since the calculated results count only fluid forces acting on the impeller vanes, and exclude all other forces on shroud plates, shaft etc, it is necessary also in the experiment to extract pure vane forces from the resultant reaction forces measured at the lower bearing.

The fluid force on the impeller vanes, $F(F_x, F_y)$, can be evaluated by the relation,

$$F = a (E_1 - E_2 - E_3 + E_4) \qquad \text{------(1)}$$

where $E(E_x, E_y)$ denotes load cell outputs in the following four sub-tests:

E_1 ; output when the whirling impeller operates as a pump, E_1 thus corresponds to total resultant force.
E_2 ; output when the rotating impeller whirls in air, E_2 thus corresponds to inertia force and coupling reaction.
E_3 ; output when a specially prepared dummy impeller (hub + consolidated shroud plate) rotates and whirls in water, E_3 thus corresponds to total force exclusive of vanes' contribution.
E_4 ; output when the rotating dummy impeller whirls in air, E_4 thus corresponds to inertia force and coupling reaction exclusive of vanes' contribution.

The following interpretation will also help understand the meaning of Eq.(1):

$a(E_1 - E_3)$; sum of mass inertia and fluid forces of vanes.
$a(E_2 - E_4)$; mass inertia force of vanes.
$a(E_1 - E_2)$; fluid forces on whirling parts submerged in water.
$a(E_3 - E_4)$; fluid forces on whirling parts submerged in water except vanes, that is, those on shrouds, shaft and seal mechanism (see Fig. 2).

Output E_1 is a function of rotational speed, ω; whirling speed, Ω; eccentricity, ε; flow rate, Q and phase angle, θ (see Fig.3); while E_2 , E_3 and E_4 are functions of ω, Ω, ε and θ. The calculation of Eq.(1) should be made using data at the same ω, Ω, ε and θ.

Test Condition

The test condition and range of parameters are listed in Table 2. From the rotordynamic consideration the whirl speed Ω corresponds to the first damped natural frequency in bending of the rotor (the critical speed). Since most troubles associated with non-synchronous rotor vibration occur at supercritical rotational speed, $\omega > \Omega$, the range of whirl speed ratio is limited to $\Omega/\omega < 1$ for positive whirl and $\Omega/\omega > -1$ for negative whirl.

Presentation of Fluid Forces

The fluid forces, F, acting on the impeller vanes are divided into two components as illustrated in Fig.3. The component normal to whirl velocity, $\varepsilon\Omega$, and directed outward is called radial force, F_r, while the component parallel and opposite to the direction of clockwise (positive) whirl is called tangential force, F_θ. A negative sign means the direction is opposite to the above definition.

Table 2 Test conditions

Impeller	ε(mm)	Ω/ω	Q
A	1.0	0.16 to 1.0	0 to max.
A	1.0	-0.16 to -1.0	0 to max.
A	2.0	0.16 to 1.0	0 to max.
B	1.0	0.16 to 1.0	0 to max.

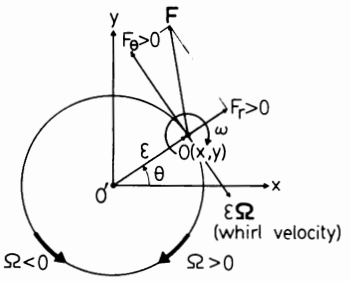

Fig.3 Radial and tangential component of fluid force

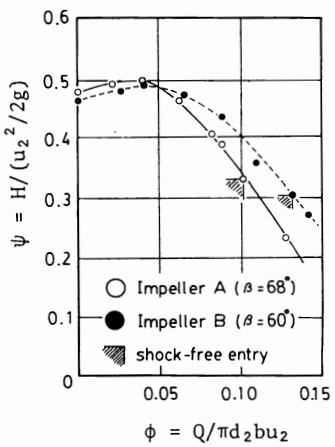

Fig.4 Characteristics of test pumps

TEST RESULTS AND DISCUSSION

Pump Characteristics

The hydraulic performance of the test pumps (impeller A and B) at steady operation is plotted in Fig.4 in non-dimensional form, where the flow coefficient, ϕ, and the head coefficient, ψ, follow the customary definitions (see notation in Table 1),

$$\phi = Q/\pi d_2 b u_2, \qquad u_2 = d_2\omega/2$$
$$\psi = H/(u_2^2/2g) \qquad \text{------(2)}$$

The total head H is the head difference between the discharge and suction pipes, where the pressure drop through the wire gauze is regarded as losses.

Shock-free entry conditions at the leading edge of the impeller vanes correspond to $\phi_{sf} = 0.101$ ($Q = 2.46$ m^3/min) for impeller A, and to $\phi_{sf} = 0.144$ ($Q = 3.49$ m^3/min) for impeller B. The machine Reynolds number of the test pump, $Re = u_2 d_2/\nu$, was about 3.7×10^6 in all test cases.

Power Spectrum

Outputs of load cells E oscillate primarily with the whirl speed Ω, but contain also other fluctuations due to mass unbalance of the impeller, rolling noise of the bearing, and countless sources of other noise. As an example, Fig.5 illustrates power spectrum density (PSD) of signal E_y at $\Omega = 10.2$ rad/s (1.63 Hz), which is calculated from 10 thousand data sampled at 1 ms intervals. The spectrum, normalized by its mean squares (MS), indicates that the disturbance due to shaft rotation is about one order of magnitude smaller than that caused by whirling motion, and that the whole phenomenon is predominantly in synchronism with the whirl frequency.

Uncertainty of Results

In experiments handling unsteady fluid forces, the scattering of data is a common problem. The cause of the scattering consists in most cases not in the uncertainly of the measuring system, but in the phenomena themselves.

Even in the present experiment, in which the impeller forces were obtained after many steps of data handling like sensing, amplification, filtration, analog recording and reproduction, A-D conversion, digital data processing and calibration, the overall uncertainty of the measured forces does not exceed five percent of their full scale magnitude, if these forces were to be applied directly to the impeller as steady forces.

From the viewpoint of error assessment, special attention must be paid to the vector calculation of Eq. (1). Figure 6 shows the relative disposition of four vectors involved in Eq.(1) at a typical test condition. Each vector is an ensemble averaged value of about one hundred data samples. On the left of the vector diagram, the scattering of each vector is demonstrated by the shaded zone at the arrowhead. The extent corresponds to the root mean squares of the scatter. Since the fluid forces on impeller vanes, F, can be evaluated by summing up four measured vectors, their uncertainty and scatter (in terms of mean squares) are also obtained by adding up those of the four vectors.

Judging from the above mentioned circumstances, the uncertainty and scatter of the evaluated final results are fairly large, reaching almost 20 to 30 percent of their full scale magnitude, respectively. Therfore, the evaluated results should be used mainly to interpret the qualitative tendency of the phenomena and to ascertain the rough magnitude of the fluid forces.

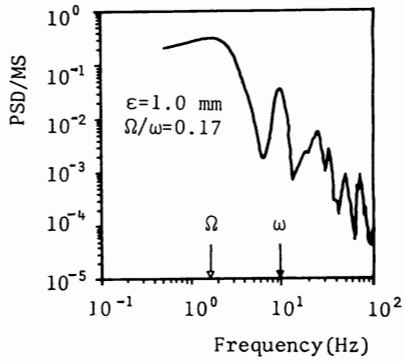

Fig. 5 Power spectrum density of load cell output; Impeller A at $\phi = \phi_{sf}$

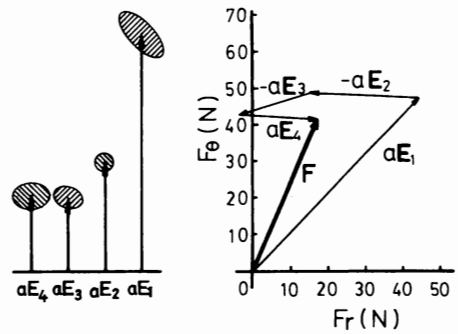

Fig.6 Relative disposition of force vectors at typical test condition; Impeller A at $\phi = \phi_{sf}$, $\varepsilon = 2.0$ mm, $\Omega/\omega = 0.83$ and $\theta = 0°$

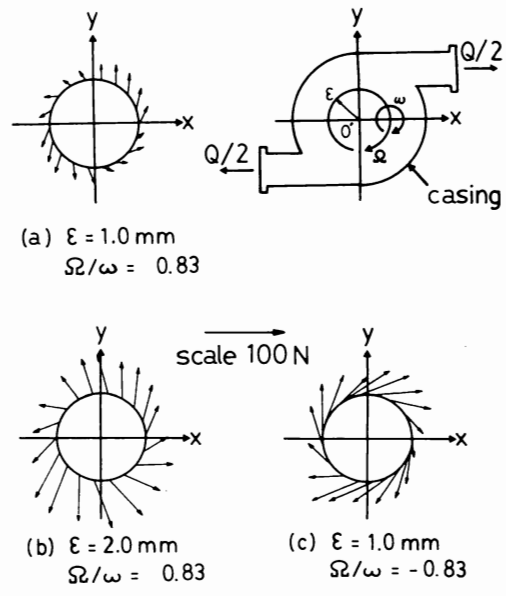

Fig.7 Fluid forces at 18 locations on the whirling orbit; Impeller A at $\phi = \phi_{sf}$

Fluid Forces on Whirling Impeller

Figure 7 illustrates fluid force vectors on impeller A at 18 equally spaced locations ($\Delta\theta = 20°$) along the whirling orbit in three test cases (a), (b) and (c). The impeller operates at shock-free entry condition, $\phi = \phi_{sf}$. The magnitude of each vector can be read by comparing with the scale of 100 N (22.5 lbf) in the figure.

In spite of precautions paid to establish azimuthally symmetric flow, the ensemble averaged force vector at each location was not sufficiently uniform. This suggests that the azimuthal distorsion caused by two discrete discharge outlets penetrated through the wire gauze into the diffuser region.

Hereafter, all results on fluid forces will be demonstrated by using the following normalized quantities.

$$f_r = \overline{F_r}/\rho Q_{\phi=1}\varepsilon\omega \quad , \quad f_\theta = \overline{F_\theta}/\rho Q_{\phi=1}\varepsilon\omega \quad \text{------(3)}$$

where, $\overline{F_r}$ and $\overline{F_\theta}$ are the averaged values of $F_r(\theta)$ and $F_\theta(\theta)$ over the orbit, ρ is the density of working fluid and $Q_{\phi=1} = \pi d_2 b u_2$.

Figure 8 shows the dependence of f_r and f_θ on the positive whirl speed ratio Ω/ω up to 1.0, when impeller A ($\beta = 68°$) operates at various flow rate; (a) for $\varepsilon = 1.0$ mm and (b) for $\varepsilon = 2.0$ mm. Results are not available for $\Omega/\omega < 0.16$, since the fluid forces in that region become so small, that the uncertainty exceeds tolerable limits. The broken lines in the figures indicate calculated result for shock-free entry condition. The comparison will be made in the succeeding section.

It is seen from Fig.8 that the radial force remains fundamentally positive, that is, the apparent mass associated with the acceleration of the impeller is positive, as it normally should be. The tendency is also obvious that the radial force is relatively insensitive to whirl speed, and that at very low flow rate it decreases rapidly as Ω/ω nears unity, where the impeller rotates solidly around its virtual center O'.

The tangential force remains also positive and increases as a whole as Ω/ω increases. This result means that the fluid force on impeller A exerts a stabilizing effect throughout the tested whirl speed range. From the extrapolation of the plotted data to lower whirl speed, however, the possibility can be predicted that the tangential force could become negative, when the whirl speed ratio nears close to zero. Therefore, the present test data do not assure the stabilizing effect of fluid forces when impeller A rotates much (more than ten times) faster than its ritical speed. The negative tangential force in this case could become large enough to excite a severe vibration, because the absolute magnitude of the forces $F_\theta = f_\theta \times \rho Q_{\phi=1}\varepsilon\omega$ increases in proportion to the square of the rotational speed ω.

Theoretical result [7] shows that fluid forces are proportional to eccentricity ε, when all other conditions are the same. If this is true in real phenomena, normalized forces given in (a) and (b) of Fig.8 must coincide thoroughly for the same flow coefficient. The obvious difference between corresponding results may be caused partly by the non-linear nature of the phenomenon, but mostly due to errors and scatter in the data. Since the results of (b) are evaluated from larger measured forces, they can claim higher certainty.

Figure 9 shows the case of impeller B ($\beta = 60°$) when it is in positive whirl with $\varepsilon = 1.0$ mm. Impeller B has a smaller vane angle and thus larger work input to the fluid than those of impeller A.

Comparison between Fig.8 and 9 reveals the important feature that the tangential force f_θ of impeller B is generally smaller and has a larger chance of becoming negative. This result suggests that impeller B does exert whirl-excitation forces at low flow rate, when it rotates faster than twice its critical speed ($\omega > 2\Omega$). As to radial force f_r no remarkable difference can be observed between the test results of two impellers.

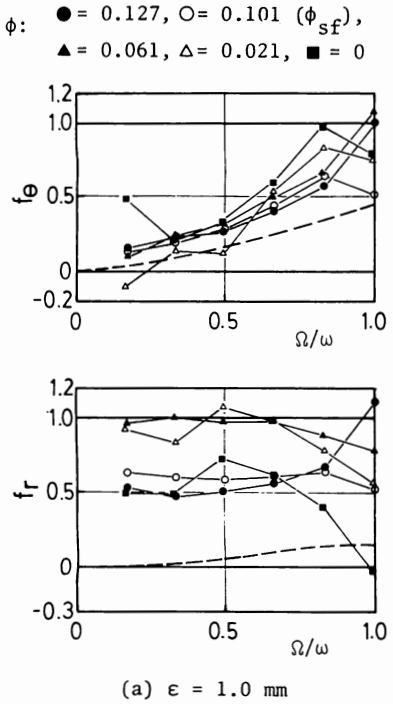

(a) ε = 1.0 mm

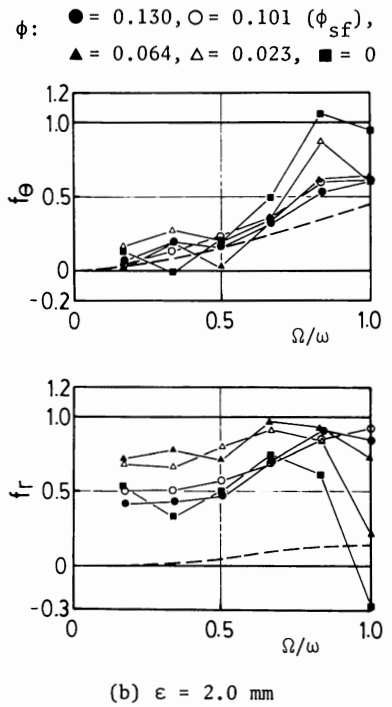

(b) ε = 2.0 mm

Fig.8 Normalized fluid forces on Impeller A in positive whirl

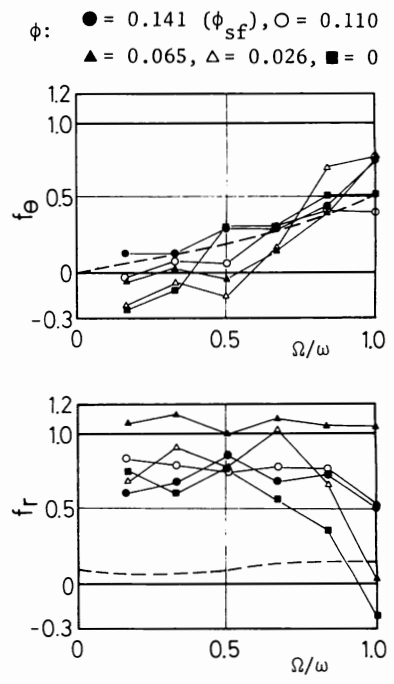

Fig.9 Normalized fluid forces on Impeller B in positive whirl for ε = 1.0 mm

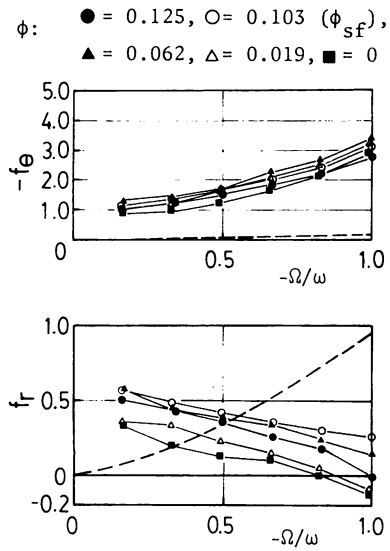

Fig. 10 Normalized fluid forces on Impeller A in negative whirl for ε= 1.0 mm

Figure 10 shows the results when impeller A is in negative whirl, $\Omega/\omega < 0$, with ε = 1.0 mm. Since the direction of whirl velocity becomes reverse, negative tangential force acts for damping in this case.

The damping effect of negative whirl is obviously much stronger than that of positive whirl. Together with the fact that negative whirl is in principle apt to decay faster than positive whirl, the experimental result predicts little chance of negative whirl.

Comparison with Theory

Fluid forces for shock-free entry conditions were calculated by the method given by Shoji and Ohashi [7]. The results are shown by broken lines in the corresponding figures.

The comparison in the case of positive whirl (Fig. 8 (a), (b) and Fig.9) indicates that the potential flow theory does predict the tangential component of measured forces quite satisfactorily, while measured radial components are several times larger than theory predicts.

In the case of negative whirl (Fig.10), the disagreement occurs in different manner. Tangential forces exerted a damping effect both in theory and experiment, but the measured damping was about ten times larger than the theoretical prediction. As to radial forces, the coincidence of magnitude is rather reasonable, while the dependence on whirl speed ratio is quite different in theory and experiment.

CONCLUSION

Fluid forces acting on a two-dimensional centrifugal impeller, which whirls in a vaneless diffuser, were measured experimentally and were compared with the corresponding theoretical results. Principal findings from two tested impellers are:

1) Fluid forces have tangential components to damp whirling motion of the rotating shaft in most cases.
2) The damping force increases as eccentricity and whirl speed increases.
3) Negative whirl has much larger damping effect than that of positive whirl.
4) At low flow rate and low whirl speed ratio, there are possibilities that the fluid forces do excert negative damping to the rotor in positive whirl.
5) Theoretical calculation can predict the tangential force in positive whirl quantitatively, while other quantities can be predicted only qualitatively.

This study will be extended further to the cases in which the impeller whirls in vaned diffuser and in a volute casing.

ACKNOWLEDGEMENT

This study was supported by Grant-in-Aid for Scientific Research by the Ministry of Education, Hitachi, Ltd. and Technical Research Institute for Integrity of Structures at Elevated Service Temperatures.

REFERENCES

1. Hergt, P. and Krieger, P., "Radial Forces in Centrifugal Pumps with Guide Vanes," Proc. Inst. Mech. Eng., Vol. 184, Pt. 3N, 1969-70, pp. 101-107.
2. Domm, V. and Hergt, P., "Radial Forces on Impellers of Volute Casing Pumps," Flow Research on Blading, Elsevier Pub. Co, 1970, pp.305-321.
3. Black, H.F., "Lateral Stability and Vibrations of High Speed Centrifugal Rotors," Dynamics of Rotors, IUTAM Symposium, Lingby, Denmark, 1974, pp.56-74.
4. Chamieh, D. and Acosta, A.J., "Dynamic Forces on a Whirling Centrifugal Rotor," Proc. 6th Conf. on Fluid Machinery, Vol. 1, Budapest, 1979, pp. 210-219.
5. Thompson, W.E., "Fluid Dynamic Excitaion of Centrifugal Compressor Rotor Vibrations," Trans. Journal of Fluids Engineering, Vol. 100, No. 1, 1978, pp. 73-78.
6. Colding-Jorgensen, J., "Effect of Fluid Forces on Rotor Stability of Centrifugal Compressors and Pumps," NASA Conference Publication 2133, 1980, pp.249-265.
7. Shoji, H. and Ohashi, H., "Fluid Forces on Rotating Centrifugal Impeller with Whirlin Motion," NASA Conference Publication 2133, 1980, pp.317-328.
8. Brennen, C.E., Acosta, A.J. and Caughey, T.K., "A Test Program to Measure Fluid Mechanical Whirl-Excitation Forces in Centrifugal Pumps," NASA Conference Publication 2133, 1980, pp. 229-235.